Int. J. Electrochem. Sci., 12 **(2017)** 2272 – 2284, doi: 10.20964/2017.03.45

International Journal of
ELECTROCHEMICAL
SCIENCE
www.electrochemsci.org

Hybrid Composites of Poly (diphenylamine sulfonic acid) and nano-Alumina for Impedimetric Humidity Sensors

Şule Dinç Zor, Hüsnü Cankurtaran[*]

Yıldız Technical University, Faculty of Science and Arts, Department of Chemistry,
34220 Davutpasa-Istanbul, Turkey
[*]E-mail: husnu3500@yahoo.com

Received: 24 December 2016 / *Accepted:* 23 January 2017 / *Published:* 12 February 2017

In this paper, nano-hybrid composites of water-soluble, conducting polymer poly (diphenylamine sulfonic acid) (PSDA) with nano-Al_2O_3 and (3-mercaptopropyl) trimethoxysilane (MPTMS) have been prepared to construct the interdigitated impedimetric type of humidity sensors. Humidity sensing characteristics of the sensors including the sensitivity, hysteresis, response/recovery time, repeatability and long-term stability were investigated. The performances of the studied sensors have been discussed by taking into consideration the film composition and applied alternating current frequency. The best results were obtained for the composite with a weight percentage of 50%Al_2O_3, which exhibits good linearity (R^2=0.9949), high sensitivity (three orders of impedance change), rapid response (55 s and 65 s at 1 kHz and 100 kHz, respectively) and recovery (155 s and 55 s at 1kHz and 100 kHz, respectively) times, low hysteresis (<4%RH), good repeatability (RSD<1%) and long-term stability (RSD<5%) in the whole relative humidity range of 10-95%. These results show that PSDA-MPTMS-Al_2O_3 nanocomposites are promising materials for impedimetric humidity sensors.

Keywords: Humidity sensor, poly (diphenylamine sulfonic acid), alumina, nanocomposite, impedance measurement.

1. INTRODUCTION

Monitoring of absolute or relative humidity in different fields such as medicine, food processing, industrial plants, agriculture and household applications is a very important issue to provide a desirable surrounding atmosphere [1-3]. In order to measure and control the ambient humidity, various types of sensors have been widely used [4]. Although the absolute humidity sensors, such as mirror-based dew/frost point hygrometers, have been used in some fields especially for trace moisture measurement, most of the commercially available humidity sensors in use are relative

humidity sensors. Relative humidity sensors are mainly based on the changes in resistance and/or capacitance properties of their sensing layers. Some of the well known sensing materials for relative humidity sensors are metal-oxide semiconductors [4–7], organic polymers [8–11], conducting polymer composites [12-15], metal-oxide/polymer composites [16-18] and other novel materials such as carbon nanotubes, graphene and nanoparticles. [19-24]. A great number of features such as electrical conductivity, good environmental and chemical stability, easy synthesis, high sensitivity/fast response to various chemicals at low temperatures makes conducting polymers eligible for detecting of various chemicals [25, 26]. One of them, poly (diphenylamine sulfonic acid) (PSDA) is a water-soluble and electrical conductive polyaniline derivative which was received attention for humidity sensing because of its facile processability in aqueous media [15, 27, 28]. However, as is well known for the other polyelectrolytes, PSDA has still some drawbacks such as low durability at extremely high and low humid atmospheres. Hence, the humidity sensing properties and durability of PSDA need to be improved by modification with the other appropriate materials such as polymers and metal oxides, as realized previously [15, 27, 29].

Among the metal oxides, alumina (Al_2O_3) has been studied as a humidity sensitive material in the literature [30-32]. The ability of alumina to sense humidity is based upon ionic conduction; the presence of an adsorbed layer of water at the surface reduces the total sensor impedance due to the increase in the ionic conductivity, as well as capacitance due to the high dielectric constant of water [33]. Nano-materials have high adsorption capacity owing to their small grain size and large specific surface area. The polymer-based nanocomposites possess remarkable properties of nanoparticles, while the polymers provide higher stability, processability and some interesting improvements [34]. Impedimetric and quartz crystal microbalance (QCM) sensors, which are based on nano-ZnO [15] and Al_2O_3 [29] composites of PSDA-MPTMS, respectively, were successfully used for the sensitive and selective determination of relative humidity. The present study was focused on the application of impedimetric type of humidity sensors of the PSDA-MPTMS-Al_2O_3 composites. For this purpose, the electrical behaviors and the response characteristics of these sensors to relative humidity were studied by impedance measurements in the frequency range of 100 Hz-1 kHz.

2. EXPERIMENTAL

2.1. Materials and methods

The electrochemical polymerization of diphenyl amine sulfonic acid (PSDA) was carried out according to our previously reported method [27]. Al_2O_3 nanoparticles (grain size <50 nm) were supplied from ABCR. Sodium salt of diphenylamine sulfonic acid, and hydrochloric acid were Aldrich products. All chemicals used in this study were of analytical grade. (3-mercaptopropyl) trimethoxysilane (MPTMS, purity 95%, ABCR) were used without further purification. Ultra pure water from a Milli-Q system (Millipore, USA) was used for preparation of all aqueous solutions.

The impedance measurements were performed using a LCR meter (HIOKI 3522-50) in a test chamber at constant temperature (20 ± 1 ^{0}C) and voltage (0.2 V), and ac frequency from 10 Hz to 100

kHz. The measurements were carried out at different relative humidity levels in the range of 10-95%RH. The various RH levels were generated by saturated salt solution method [35] and controlled by a Carl Roth P330 capacitive type of commercial humidity sensor. This humidity sensor has a 0-99% relative humidity measuring range with an accuracy of ± 3%RH. A flow controller (Aalborg SDPROC) and two AFM 26 mass flow meters were also used to obtain different flowing humid atmospheres in the measurement of transient time and repeatability. High purity nitrogen gas was flushed into the chamber for the regeneration of the sensors which had been exposed to humid atmosphere. Infrared spectra of the nanocomposite materials were recorded with a Perkin Elmer Spectrum One FT-IR spectrometer. Scanning electron microscope (SEM) images of the prepared sensor films were characterized using a Philips XL 30-ESEM-FEG/EDAX instrument.

2.2. Preparation of PSDA-MPTMS-Al_2O_3 nanocomposites

For the preparation of PSDA-MPTMS-Al_2O_3 nanocomposite sol-gels, 80 µL of 10 wt% PSDA in 0.1 M HCl solution, 2 µL of pure MPTMS and the desired amount of nano-Al_2O_3 were mixed thoroughly by ultrasonication for 15 min [15, 29]. Three different PSDA-MPTMS-Al_2O_3 nanocomposites were prepared containing 10, 30 and 50 wt% of Al_2O_3, which are designated as NC10, NC30 and NC50, respectively. For comparison, PSDA-MPTMS composite (CP) was prepared by the same procedure without Al_2O_3 nanoparticles.

2.3. Fabrication of the humidity sensors

5 µL of as-prepared sol-gel solutions were pipetted onto the circular silver coated copper interdigitated electrode on epoxy based substrate [15, 27] and the films were allowed to dry at room temperature. And finally, the coated electrodes were heated at 105 ^{0}C for 2 hours in an oven.

3. RESULTS AND DISCUSSION

3.1. Structural characterizations

The FTIR spectra of nano-sized Al_2O_3, PSDA and PSDA-MPTMS-Al_2O_3 nanocomposite are given in Fig. 1.a, b and c, respectively. The broad bands at 3350 and 1640 cm^{-1} in Fig.1.a are attributed to the hydrogen bonded water adsorption by Al_2O_3. The other intense broad band centered at 843 cm^{-1} is due to the stretching vibration of Al-O-Al bond [36]. As previously reported, the peak at 1176 cm^{-1} for PSDA (Fig.1.b), which corresponds to the symmetric vibration of free –S=O group of PSDA, was shifted to 1217 cm^{-1} for PSDA-MPTMS-Al_2O_3 composite (Fig. 1.c) [29]. In addition, the asymmetric vibration of free –S=O group of PSDA at 1370 cm^{-1} was appeared as a more intense peak at 1366 cm^{-1}. The intensity of the benzenoid and quinoid rings stretching peaks of pure PSDA at 1444, 1498 and 1594 cm^{-1} decreases in PSDA-MPTMS-Al_2O_3 composite. The latter one is collided with the bending vibration of water at 1627 cm^{-1}. As shown in Fig.1.c, the strongest bands of the spectrum at

3343 and 1627 cm^{-1} indicate the presence of the hydrogen bonded –OH functionality, which belongs to the – SO_3H, -Si-OH and -Al-OH groups, and the high water adsorption capacity of the composite. The peaks at 1124 and 872 cm^{-1} might be indicative for the formation of Si–O–Al bonds [37, 38]. In the spectrum of PSDA-MPTMS-Al_2O_3 composite, the weak absorption band at around 2500 cm^{-1} may be attributed to the presence of free –SH group [39]. It was difficult to identify the peak at 1737 cm^{-1}, however, it may be assigned to the adsorbed CO_2 molecules concerning the bridged carbonate ions or the strongly perturbed carbon dioxide molecules [40].

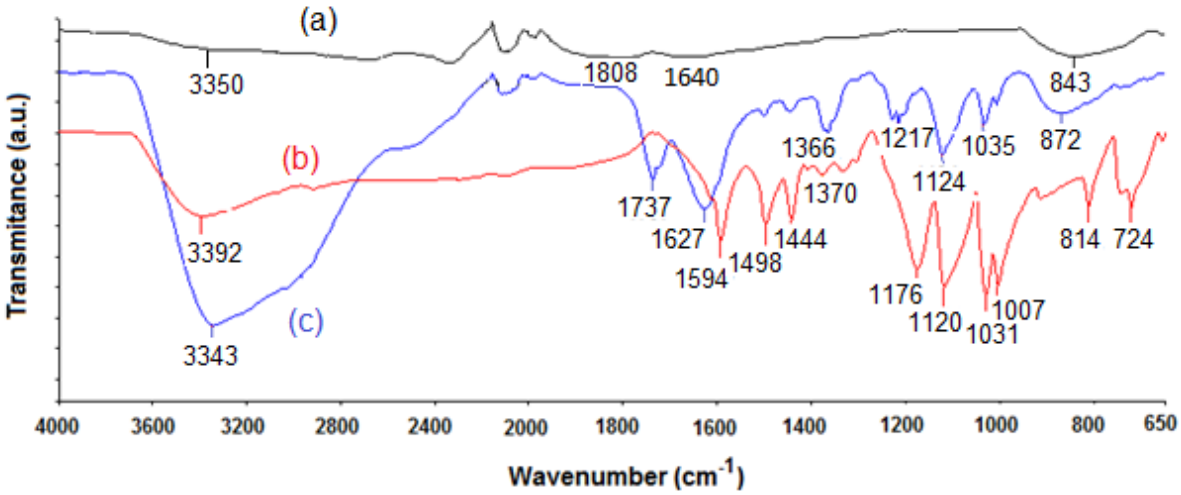

Figure 1. FTIR spectra of (a) Al_2O_3 nanoparticles, (b) PSDA and (c) PSDA-MPTMS-Al_2O_3 nanocomposite (NC50).

3.2. Morphology

The morphology and surface properties of PSDA, PSDA-MPTMS and the composites of PSDA-MPTMS with nano powder of ZnO and Al_2O_3 had been discussed in our previous studies [15, 29]. As confirmed by SEM images in Fig. 2.a, the surface of the interdigitated electrode was covered with the PSDA-MPTMS film as uniformly dispersed micro-droplets in the highly ordered polysilane network. For PSDA-MPTMS-Al_2O_3 composite, it is shown from Fig. 2.b that Al_2O_3 nanoparticles and the other constituents were homogeneously distributed in the composite matrix. The Al_2O_3 nanocomposite films were composed of nano grains and no phase separation or aggregation was observed. It is likely to have highly porous surface area for the facile adsorption of water molecules into the composite film. Due to the water soluble nature of PSDA, MPTMS was added into the nanocomposites to adjust the hydrophilicity and the stability of the sensing layer, gaining the highly ordered and water-durable films for the incorporation of the other constituents in the composite. Taking into consideration both the FTIR and SEM results, some interactions may be foreseen in the sensor materials as shown in Fig. 3. To sum up, incorporation of MPTMS and alumina enhance the surface properties and water durability of the PSDA based films, and further studies have confirmed this finding [12, 22, 29].

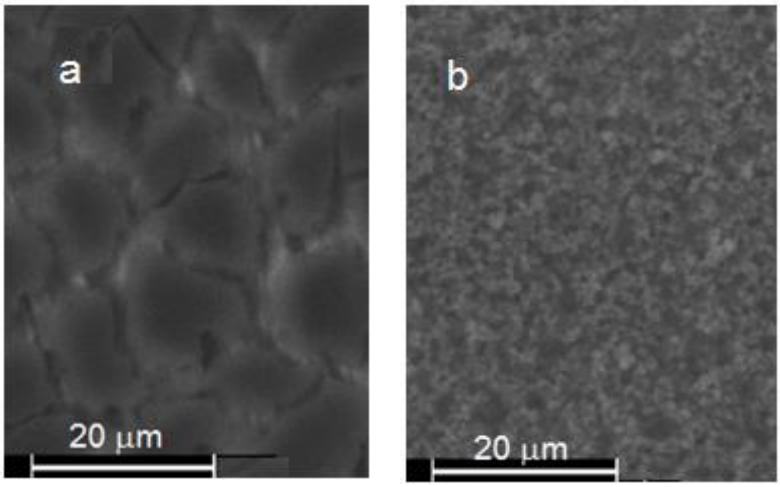

Figure 2. SEM images of (a) PSDA-MPTMS and (b) PSDA-MPTMS-Al_2O_3 nanocomposite.

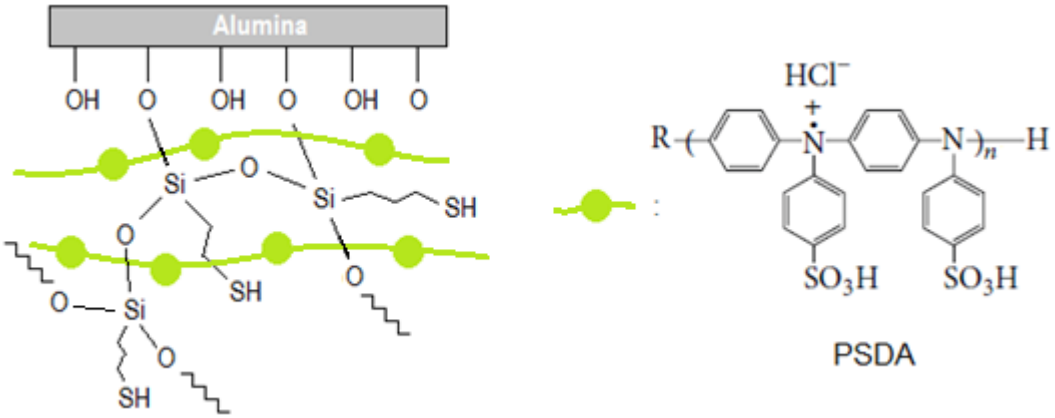

Figure 3. Schematic illustration of some possible interactions among the film components.

3.3. Humidity sensing properties of Composites

3.3.1. Complex impedance characteristics and sensing behaviors

The complex impedance spectra of NC50 composite were given in Fig. 4 to demonstrate the general electrical characteristic of PSDA-MPTMS-Al_2O_3 nanocomposites at low, moderate and high humid atmospheres. In order to make better comparison in the same graph, some plots were multiplied by appropriate factors (in brackets) and some points at low frequencies were omitted. The impedance characteristic of CP composite is well known from our previous study [15] and not given here again. As obvious from Fig. 4, NC composite films have high impedance values at low humidity level in the frequency range studied. At moderate humidity values, semicircles existed in high frequency range with or without a straight line in low frequency range, indicating the decrease in their impedance values with water adsorption. At highest humidified atmosphere (95%RH), the semicircle is almost disappeared and a straight line predominates in the spectra within the large frequency range studied, indicating the purely mass transfer controlled conduction mechanism. The depressed semicircles, and

straight lines with slopes smaller than 1 under high humidity levels have been considered to be related with highly porous structure of the films. In this case, the composite films may be regarded as constant phase element (CPE) [41, 42].

Bode plot is another useful representation for gaining more information about the frequency dependency of impedance. In Bode diagrams, the absolute value of the total impedance (|Z|) or the imaginary part of the impedance and the phase angle is plotted as a function of the angular frequency ($w=2\pi f$) [43]. In log|Z| versus log$w$ plots, extrapolation of the linear section of the curve at mid-frequency region to log$w$ = 0 gives log(1/C), where C is the double layer capacitance. As apparently shown from Bode plots in Fig. 5.a, b and c, the impedance of NC50 sensor and its resistive and capacitive components exhibit very strong dependency with the applied frequency and humidity, especially at low RH and high frequency. At high humidity levels, variation of impedance and resistance with frequency was insignificant, whereas the capacitive reactant changed slightly. Impedance is mainly determined by the capacitive reactant at low humidity levels, i.e., the capacitive reactant is higher than resistance. It is also interesting to note that the resistance of NC50 sensor is higher under moderate humidity levels (60%RH in Fig. 5.b) than that of low humidity levels (15%RH in Fig.5.b) in a large frequency range down to 1 kHz. It means that the capacitive reactant mainly determines the total impedance response to humidity in almost all frequency range. In fact, as seen from these figures, the change in capacitive reactant was nearly four orders of magnitude between 15%RH and 95%RH, while this change was about three orders of magnitude for impedance and resistance. These observations confirm that the NC50 sensor mainly behaves as a capacitor, whereas the main charge transfer mechanism at low frequency range is based on the diffusional mass transfer mechanism of ionic species. As shown from the plots in Fig.5.b, the capacitance increases, i.e., 1/C decreases with the humidity increase. Consequently, the results confirmed that the porosity of the films is an important factor on the sensor response. The sensitivity of the films specifically increases at low and moderate humidity range with the increase of Al_2O_3 percentage in the composite. The effect of Al_2O_3 on the humidity sensing performance of NC composites has been studied in detail (vide infra).

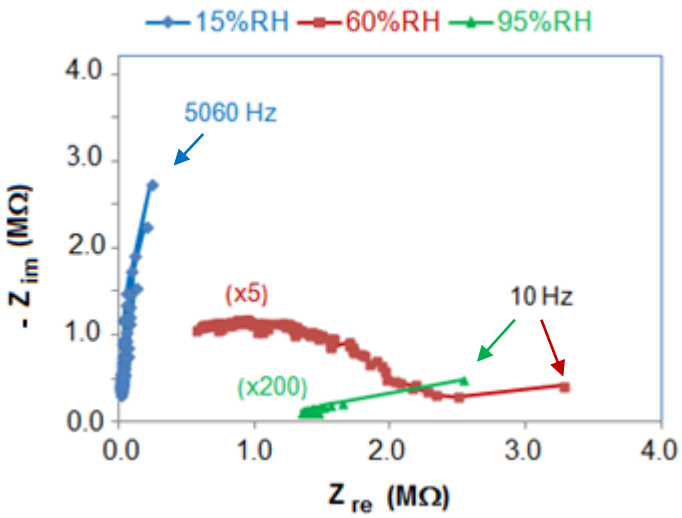

Figure 4. Complex impedance spectra (Nyquist plot) of NC50 nanocomposite at low, moderate and high humidity atmospheres.

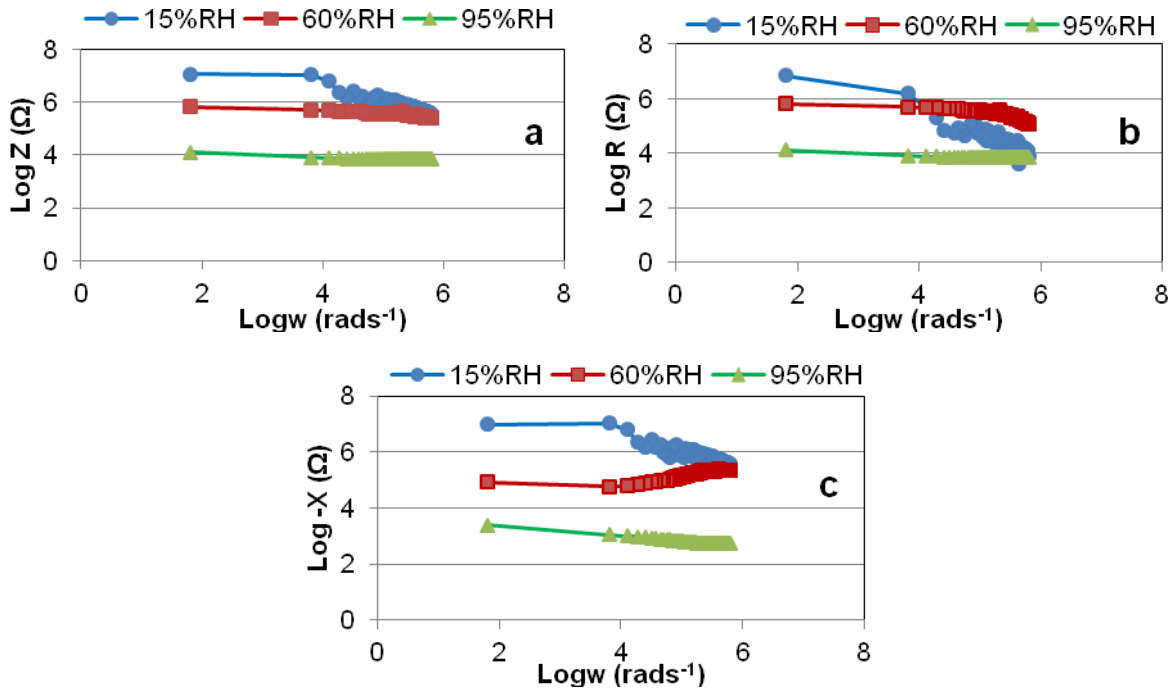

Figure 5. Bode plots for NC50 nanocomposite at low, moderate and high humidity atmospheres.

3.3.2. The Effect of Al_2O_3 *on Humidity Sensing Characteristics*

The effect of the amount of Al_2O_3 nanoparticles on the humidity sensing behaviors of the nanocomposites was measured at various RHs, and the results are shown in Fig. 6. As shown from the figure, the decrease in the impedance of the sensors with the increase in humidity indicates their humidity sensitivity. The impedance of the PSDA-MPTMS (CP) decreased from 4.0×10^4 kΩ to 16 kΩ with an increase in RH from 10% to 95%. However, as shown from the curve in Fig. 6, pure CP film did not show high sensitivity at low and moderate humidity range from ca. 10%RH to 50%RH. It is obviously seen that the humidity sensitivity at low and moderate humidity ranges is increased with the addition of Al_2O_3 into the composite. This behavior should be due to the increased porosity and surface area of the film with the increase of nano-Al_2O_3 percentage. The impedance of PSDA-MPTMS-Al_2O_3 (NC50) changes from 9.5×10^3 kΩ to 8.5 kΩ with a good linear response (R^2=0.9949) when RH increases from 10 to 95%, that its impedance changed approximately by more than three orders of magnitude. From the results obtained, we can infer that Al_2O_3 in the nanocomposite plays an important role on the sorption mechanism of water molecules [15, 29]. Because of its linear response with a high sensitivity in a wide humidity range, NC50 nanocomposite was chosen for further studies to investigate the other sensing performance parameters such as response-recovery times, hysteresis, and repeatability.

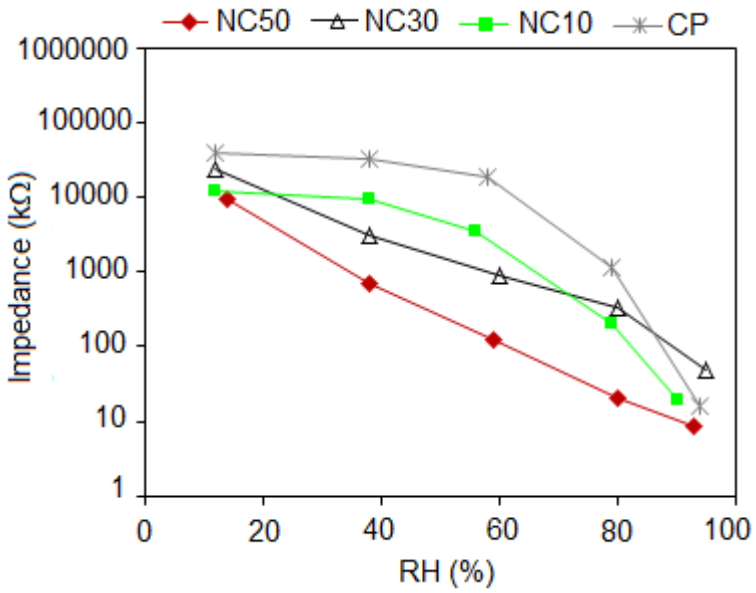

Figure 6. Humidity sensing response of NC10, NC30, NC50 and CP measured at 0.2 V, 1 kHz.

3.3.3. The Effect of Frequency on Response

The effect of the applied frequency on the sensor impedance was measured in a frequency range of 100 Hz-1 kHz. It can be obviously seen for NC50 sensor from Fig. 7, the magnitude of the applied frequency affects the impedance more strongly at low RHs rather than at high RHs. At low and moderate humidity atmosphere, the sensitivity decreases greatly when the frequency increases.

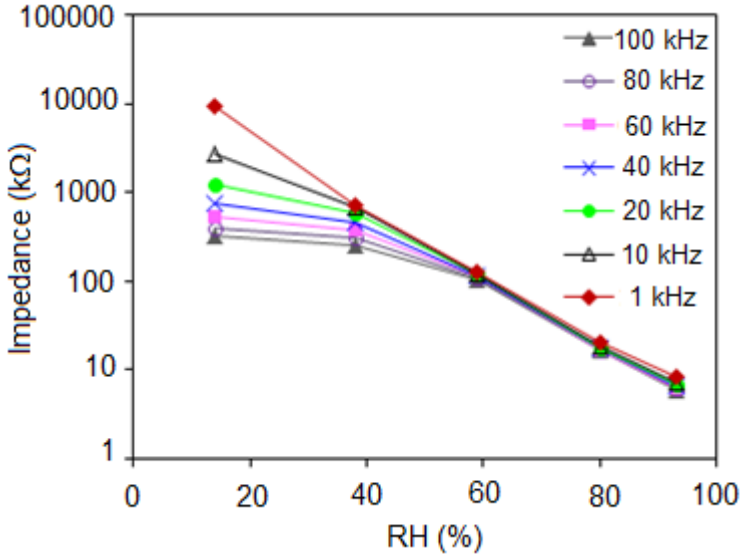

Figure 7. Influence of applied frequency on the impedance of NC50 nanocomposite in the humidity range of 10-95%RH.

This result is in agreement with the previous studies in literature [15, 17, 44]. The Al_2O_3 nanocomposites and CP exhibit almost identical sensing behaviors towards applied frequencies [15]. For NC50 sensor, the best sensitivity and linearity was obtained at 1 kHz, and the applied frequency

was thus kept constant at 1 kHz for further studies. As shown also from Fig. 6, the other sensors studied did not give the linear responses against humidity even at 1 kHz.

3.3.4. Repeatability, Hysteresis, and Long-Term Stability

Fig. 8 illustrates a typical time dependent response of NC50 sensor when it was exposed to a humidity cycle between 10%RH and 95%RH. As can be seen from the figure, the humidity sensing process is extremely reversible and repeatable for the nanocomposite sensor. The relative standard deviations in impedance values at low and high humidity levels in these experiments were less than 1%. Whole sensors studied have good repeatability. But, because of their low sensitivity and non-linear response behavior, repeatability properties of NC10 and NC30 composite films were not further studied in detail.

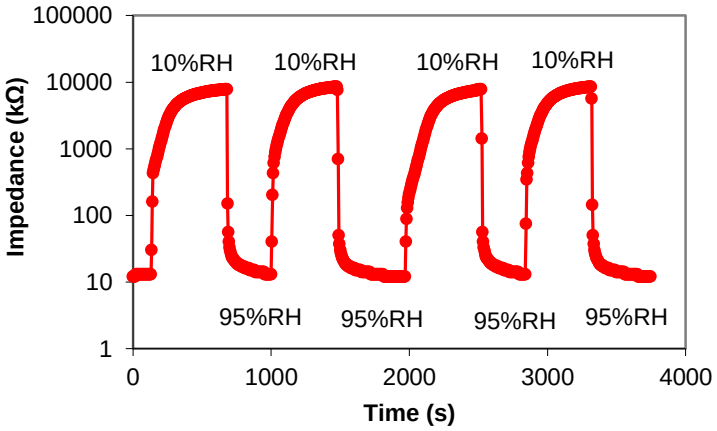

Figure 8. Repetitive response of NC50 nanocomposite sensor to successive exposure cycles of 10%RH and 95%RH, measured at 0.2 V and 1 kHz.

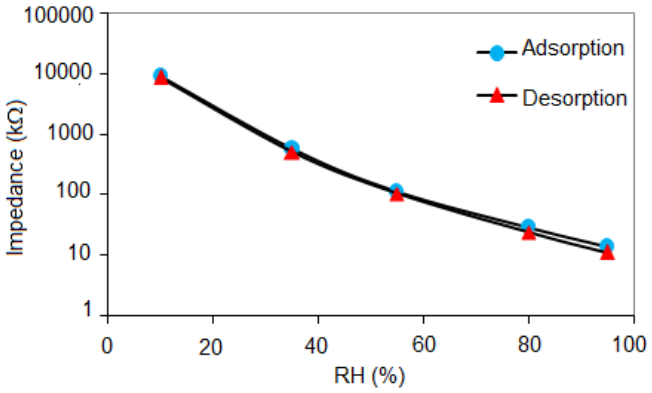

Figure 9. Hysteresis characteristic of NC50 nanocomposite measured by stepwise humidity adsorption and desorption route between 10%RH and 95%RH, measured at 0.2 V and 1 kHz.

Hysteresis curves inform about adsorption and desorption characteristics of humidity sensors. Fig. 9 reveals the hysteresis properties of NC50 sensor. As shown from the curves, it has a low hysteresis (<4%RH) in a large humidity range. Conversely, as we know from our previous work, CP

based sensor shows relatively high hysteresis at moderate and high humidity levels (data not shown, ref 15). The long term-stability of NC50 sensor was satisfactory even in the harsh conditions such as high RHs (RSD<5%). These studies were achieved by measuring their impedance repeatedly at the same humidity every 7 days for 1 month. The results obtained are in accordance with our previous works and confirm the stability of the impedimetric NC sensors [15, 29].

3.3.5. Response and Recovery Time

The response and recovery times of the humidity sensors have been found from the signal measurements during the exposing the humidity between the desired low and high levels. The response or recovery time has been defined as the time required for achieving 90% of the steady state equilibrium response when the humidity is increased or decreased between two different humidity levels, respectively. The transient impedance responses of NC50 sensor are shown in Fig. 10. The response (adsorption) and recovery (desorption) times at 1 kHz ac frequency were obtained to be 55 s and 155 s when the humidity was changed from 10%RH to 95%RH and then from 95%RH to 10%RH, respectively.

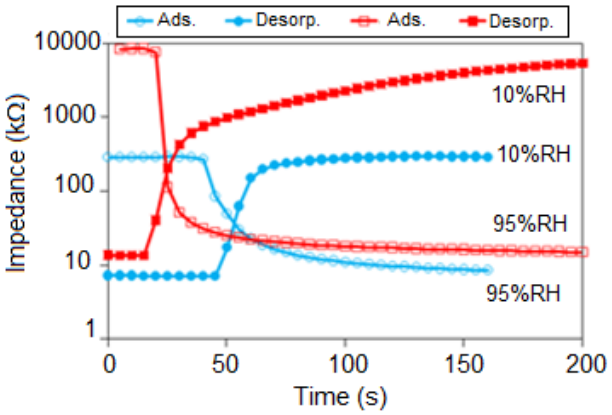

Figure 10. Transient response of NC50 sensor to humidity adsorption and desorption cycles between 10%RH and 95%RH. Blue and red curves designate the measurements at 100 kHz and 1 kHz, respectively.

At 100 kHz ac frequency, the response and recovery times were found to be 65 s and 55 s, respectively. As known from our previous studies for the humidity sensors based on the copolymer of PSDA with poly (ethylene glycol) (PEG) and ZnO composites of PSDA-MPTMS [15, 27], such frequency dependent sensitivity, response and recovery behaviors of NC50 sensor are not surprising. It is obvious that the application of low ac frequency leads to higher electrostatic attractive forces between water molecules and NC composite film and consequently higher sorption and lower desorption rates. It might be kept in mind that desorption of more water molecules, adsorbed in the inner site of the sensitive film, might takes longer time at low frequency. Because of varying film thickness on and between the digits (thickness of the digits was 20 μm), we could not mention about the exact thickness of the studied films. However, the average film thickness changes in the order of

CP<NC10<NC30<NC50. It is expected that better response and recovery times could be obtained for the thinner NC50 films. These results indicate that the response and recovery characteristic of NC50 sensor is adequate for practical use and may be enhanced by using the appropriate film thickness and frequency.

3.3.6 Comparison of performance of PSDA-MPTMS-Al_2O_3 composite with other polymer/metal oxide composite used in the humidity sensors

The performance of PSDA-MPTMS-Al_2O_3 composite (NC50) was compared with some of the other polymer/metal oxide composites in Table 1. As shown from Table 1, the sensing properties of the proposed sensor, in terms of response/recovery time, measurable humidity range, sensitivity and hysteresis, are comparable to those of the other humidity sensors based on polymer-metal oxide composites [10, 12, 14-18, 44-50].

Table 1. Some performance characteristics of humidity sensors based on polymer/metal oxide composites in literature.

Material*	Response Time (s)	Recovery Time (s)	Hysteresis (%)	Order of signal change	Sensing Range (%RH)	Ref.
PANI/WO_3	4-5	10	-	-	10-95	10
PPy/TiO2	40	20	Low	2	30-90	12
PANI/Mn_3O_4	15	-	Low	1	20-90	14
PSDA-MPTMS-ZnO	90	60	<4	>3	12-95	15
$BaTiO_3$/polymer RMX	15	120	3	2	33-98	16
SiO_2/poly(AMPS)	60	120	Low	4	30-90	17
POA/SnO_2	87	13	4	1	20-100	18
TiO_2/PPy/ PMAPTAC	30	45	2	~4	11-91	44
POA/WO_3	50	49	6	1	25-95	45
PDMA/WO_3	27	136	~5	1	23-84	46
PPy/αFe_2O_3	-	-	-	-	~20-80	47
PMAPTAC/SiO_2	60	120	2	3	10-90	48
PANI/SnO_2	26	30	-	1	5-95	49
PSS/ZnO	2	2	<2	4	11-97	50
PSDA-MPTMS-Al_2O_3	55 (1 kHz) 65 (100 kHz)	155 (1 kHz) 55 (100 kHz)	<4	3	10-95	This work

*Abbreviations: PANI: Polyaniline; Ppy: Polypyrrole; RMX: Quaternary acrylic resin; AMPS: Poly(2-acrylamido-2-methylpropane sulfonate); POA: Poly(o-anisidine); PMAPTAC: Poli[3-(methacrylamino)propyl] trimethyl ammonium chloride; PDMA: Poly(2,5-dimethoxyaniline); PSS: Polystyrenesulfonate

4. CONCLUSION

In summary, PSDA-MPTMS-Al_2O_3 nanocomposites for measuring relative humidity in 10–95%RH range have been presented. High linear sensitivity in this humidity range was achieved when PSDA-MPTMS with 50 wt% Al_2O_3 was used. The response and recovery times of this sensor were 55 s and 155 s at 1 kHz and 65 s and 55 s at 100 kHz, respectively. Besides, the sensor exhibits negligible hysteresis (<4%RH), good repeatability (RSD<1%) and long-term stability (RSD<5%) in a wide humidity range. While the incorporation of Al_2O_3 improves the porosity and surface properties of the composites for better sensitivity, MPTMS is considered to be beneficial for the structural stability of the sensors, especially at high humidity levels. Thanks to their persuasive electrical and humidity sensing properties, PSDA-MPTMS-Al_2O_3 composites would be suggested as impedimetric humidity sensing materials.

ACKNOWLEDGEMENTS
This research was supported by Yildiz Technical University Scientific Research Projects Coordination Department. Project Number: 2011-01-02-DOP05.

References

1. N. Yamazoe, Y. Shimizu, *Sensor Actuators* 10 (1986) 379–398.
2. E. Traversa, *Sens Actuators B Chem*. 23 (1995) 135-156.
3. H. Farahani , R. Wagiran, M. N. Hamidon, *Sensors* 14 (2014) 7881-7939.
4. Z. Chen, C. Lu, Sensor Lett. 3 (2005) 274-295.
5. S. P. Yawale, S. S. Yawale, G. T. Lamdhade, *Sens Actuators A* 135 (2007) 388-393.
6. D. Li, Y. Li, F. Li, J. Zhang, X. Zhu, S. Wen, S. Ruan, Ceram. Int. 41 (2015) 4348-4353.
7. Y. Qiu, S. Yang, *Adv. Funct. Mater.* 17 (2007) 1345–1352.
8. B. Adhikari, S. Majumdar, *Prog. Polym. Sci.* 29 (2004) 699–766.
9. Y. Li, B. Y.Ying, L. J.Hong, M. J.Yang, *Synth. Met.* 160 (2010) 455–461.
10. R. Nohria, R. K. Khillan, Y.Su, R.Dikshit, Y.Lvov, K.Varahramyan, *Sens Actuators B* 114 (2006) 218–222.
11. K. H. Choi, M. Sajid, S. Aziz, B. Yang, *Sens Actuators A* 228 (2015) 40–49.
12. P. G. Su, L. N. Huang, *Sens Actuators B* 123 (2007) 501–507.
13. N. Parvatikar, S. Jain, S. Khasima, M. Revansiddappa , S. V. Bhoraskar, M. V. N. Ambika Prasad, *Sens Actuators B* 114 (2006) 599–603.
14. M. L. Singla, S. Awasthi, A. Srivastava, *Sens Actuators B* 127 (2007) 580–585.
15. S. D. Zor, H. Cankurtaran, *Journal of Sensors* (2016), Article ID 5479092.
16. J. Wang, Q. Lin, R. Zhou, B. Xu, *Sens Actuators B* 81 (2002) 248-253.
17. P. G. Su, W. Y. Tsai, *Sens Actuators B* 100 (2004) 417–422.
18. D. Patil, P. Patil, Y. K. Seo, Y. K. Hwang, *Sens Actuators B* 148 (2010) 41–48.
19. K. P. Yoo, L. T. Lim, N. K. Min, M. J. Lee, C. J. Lee, C. W. Park, *Sens Actuators B* 145 (2010) 120–125.
20. D. Zhang, J. Tong, B. Xia, *Sens Actuators B* 195 (2014) 66–72.
21. V. K. Tomer, S. Duhan, A. K. Sharma, R. Malik, S. P. Nehra, S. Devi, *Colloids Surf. A Physicochem. Eng. Asp.* 483 (2015) 121–128.
22. X. Feng, W. Chen, L. Yan, *Sens Actuators B* 215 (2015) 316–322.
23. J. Wang, M. Y. Su, J. Q. Qi, L. Q. Chang, *Sens Actuators B* 139 (2009) 418–424.

24. D. Zhang, H. Chang, P. Li, R. Liu, Q. Xue, *Sens. Actuators B* 225 (2016) 233–240.
25. H. Bai, G. Shi, *Sensors* 7 (2007) 267-307.
26. H. Yoon, *Nanomaterials* 3 (2013) 524-549.
27. H. Cankurtaran, Ö. Yazici, Ş. Dinç, F. Karaman, *Int. J. Electrochem. Sci.* 8 (2013) 3265–3278.
28. F. Hua, E. Ruckenstein, *J Polym Sci: Part A: Polym. Chem.* 42, 9 (2004) 2179–2191.
29. S. D. Zor, H. Cankurtaran, *Int. J. Electrochem. Sci.* 11 (2016) 7976-7989.
30. Z. Chen, C. Lu, *Sensor Lett.* 3 (2005) 274–295.
31. L. Z. Yuan, C. S. Shuo, W. J. Chi, L. Yi, *Chinese Sci. Bull.* 53 (2008) 183-187.
32. L. Yao, M. Zheng, H. Li, L. Ma, W. Shen, *Nanotechnology* 20, 39 (2009) 395501.
33. E. C. Dickey, O. K. Varghese, K. G. Ong, D. Gong, M. Paulose, C. A. Grimes, *Sensors* 2 (2002) 91-110.
34. X. Zhao, L. Lv, B. Pan, W. Zhang, S. Zhang, Q. Zhang, *Chem. Eng. J.* 170 (2011) 381–394.
35. L. Greenspan, *J. Research NBS-A* 81A 1 (1977) 89-96.
36. T. M. H. Costa, M. R. Gallas, E. V. Benvenutti, J. A. H. da Jornada, *J. Phys. Chem. B* 103 (1999) 4278-4284.
37. S. F. Wang, Y. F. Hsu, T. C. K. Yang, C. M. Chang, Y. Chen, C. Y. Huang, F. S. Yen, *Mater. Sci. Eng. A* 395 (2005) 148–152.
38. G. Mondin, M. R. Lohe, F. M. Wisser, J. Grothe, N. M. Noriega, A. Leifert, S. Dörfler, A. Bachmatiuk, M. H. Rümmeli, S. Kaskel, *Electrochim. Acta* 114 (2013) 521– 526.
39. R. M. Silverstein, F. X. Webster, D. J. Kiemle, Spectrometric Identification of Organic Compounds, John Wiley & Sons, Inc., NJ., USA (2005).
40. V. A. Ivanov, A. Pieplu, J. C. Lavalley, P. Nortier, *Appl. Catal. A: General* 131 (1995) 323-334.
41. P. M. Faia, C. S. Furtado, A. J. Ferreira, *Sens Actuators B* 107 (2005) 353–359.
42. Q. Lin, Y. Li, M. Yang, *Sens Actuators B*, 171– 172 (2012) 309– 314.
43. C. H. Hamann, A. Hamnett, W. Vielstich, *Electrochemistry*, Wiley-VCH,Weinheim, Germany, 2nd edition, 2007.
44. P. G. Su, C. P. Wang, *Sens Actuators B* 129 (2008) 538–543.
45. D. Patil, Y. K. Seo, Y. K. Hwang, J. S. Chang, P. Patil, *Sens Actuators B* 128 (2008) 374–382.
46. D. Patil, Y. K. Seo , Y. K. Hwang, J. S. Chang, P. Patil, *Sens Actuators B* 132 (2008) 116–124.
47. K. Suri, S. Annapoorni, A. K. Sarkar, R. P. Tandon, *Sens Actuators B* 81 (2002) 277-282.
48. P. G. Su, S. C. Huang, *Sens Actuators B* 105 (2005) 170-175.
49. S. K. Shukla, S. K. Shukla, P. P. Govender, E. S. Agorku, *Microchim Acta* 183 (2016) 573–580.
50. Y. Li, M. J. Yang, Y. She, *Talanta* 62 (2004) 707–712.